Iridium Cyclooctene Complex Forms a Hyperpolarization Transfer Catalyst Before Converting to a Binuclear C-H Bond Activation Product Responsible for Hydrogen Isotope Exchange

Wissam Iali, Gary G. R. Green, Sam Hart, Adrian C. Whitwood and Simon B. Duckett*

Centre for Hyperpolarization in Magnetic Resonance, University of York, York, YO10 3NR, UK.

Supporting Information Placeholder

$[IrCl(COE)_2]_2$ (**1**) reacts with pyridine and H_2 to form crystallographically characterized $IrCl(H)_2(COE)(py)_2$ (**2**). **2** undergoes pyridine loss to form 16-electron $IrCl(H)_2(COE)(py)$ (**3**) with equivalent hydride ligands. When this reaction is studied with *para*hydrogen, **1** efficiently achieves the hyperpolarization of free pyridine (and nicotinamide, nicotine, 5-aminopyrimidine and 3,5-lutudine) via signal amplification by reversible exchange (SABRE) and hence reflects a simple and readily available precatayst for this process. **2** reacts further over 48 hrs at 298 K to form crystallographically characterized $(Cl)(H)(py)(\mu\text{-}Cl)(\mu\text{-}H)(\kappa\text{-}\mu\text{-}NC_5H_4)Ir(H)(py)_2$ (**4**). This dimer is shown to be active in the hydrogen isotope exchange process that is used in radiopharmaceutical preparations. Furthermore, while $[Ir(H)_2(COE)(py)_3]PF_6$ (**6**) forms on addition of $AgPF_6$ to **2**, its stability precludes its efficient involvement in SABRE.

Nuclear Magnetic Resonance (NMR) spectroscopy is used widely in chemistry and biochemistry to characterize materials, while in medicine magnetic resonance imaging is used to probe disease. Both methods suffer from low sensitivity, that can be overcome by employing hyperpolarization as exemplified by optical pumping[1], dynamic nuclear polarization (DNP),[2] and *para*hydrogen (p-H_2).[3] The resulting molecules are starting to be featured as disease probes in clinical diagnosis.[4]

*Para*hydrogen induced polarization (PHIP) involves the chemical transfer of two hydrogen atoms into a suitable acceptor.[5] This approach was pioneered by Weitekamp[3], Eisenberg[6] and Bargon.[7] Examples of hydrogen acceptors include organic scaffolds leading to fumaric acid[8] and inorganic complexes such as Vaska's complex.[9] One related PHIP approach, is known as signal amplification by reversible exchange (SABRE).[10] Like PHIP, it is able to hyperpolarize a target in seconds, but crucially it no longer involves the incorporation of p-H_2 into it. Instead, it utilizes a metal complex to simultaneously bind p-H_2 and the hyperpolarization target. When so assembled, polarization flows from the p-H_2 derived spins at low magnetic field to those of the target, which upon dissociation can be detected with high sensitivity.

Crabtree's catalyst, $[Ir(COD)(PCy_3)(py)][BF_4]$ (COD = cyclooctadiene, Cy = cyclohexyl, and py = pyridine) exhibits roles in hydrogenation[11] and hydrogen isotope exchange (HIE)[12] where it is used in the production of labelled compounds and radiopharmaceuticals.[13] When it reacts with p-H_2 and py though it forms the active magnetization transfer catalyst $[Ir(H)_2(PCy_3)(py)_3][BF_4]$.[14] Interrogation of the free pyridine's ^1H NMR signals after magnetization transfer revealed signal enhancements of >100 fold in the corresponding ^1H, ^{13}C and ^{15}N NMR spectra. This process has now been refined to extend the level of signal gain[15-18], the range of applications[19, 20], the nuclei that can be polarized,[21-25] and the classes of substrates that can be employed.[26-28] So far IrCl(COD)(IMes)[29] (IMes = 1,3-bis(2,4,6-trimethylphenyl)imidazole-2-ylidene)[4] reflects one of the better SABRE catalysts because its ligand exchange rates match those of the spin-spin couplings associated with polarization flow, but slow catalyst activation can be a problem.[30, 31] We set out here to develop a rapidly activating and readily available air-stable precursor for SABRE and now describe the ensuing observations.

Initially, the COD ligand of IrCl(COD)(IMes) was replaced with cyclooctene (COE), in the form of $IrCl(COE)_2(IMes)$,[32] by adding IMes to $[IrCl(COE)_2]_2$ (**1**). $IrCl(COE)_2(IMes)$ proved unstable, although $[Ir(H)_2(IMes)(py)_3][Cl]$ forms upon reaction with py and H_2. As a consequence, we treated a tetrahydrofuran (THF-d_8) solution of **1** with py and H_2 alone. **1** rapidly formed $IrCl(H)_2(\eta^2\text{-}COE)(py)_2$ (**2**), as detailed in Figure 1.

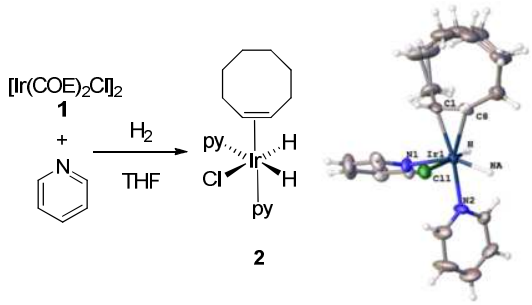

Figure 1: Reaction scheme for the formation of $IrCl(H)_2(COE)(py)_2$ (**2**) from **1** and the associated ORTEP for **2**.

The COE ligand of **2** binds in an η^2 fashion, *trans* to one of two inequivalent py ligands, while its hydride ligands lie *trans* to chloride and py. The py-N_1-Ir-alkene-centroid bond angle in **2** is 101.6(6)° while the py-iridium-chlorine bond angles are 91.1(3)° and 92.4(3)°. Its structure is therefore close to octahedral, although the py ligand *cis* to the alkene is slightly displaced away from the equatorial plane. The corresponding alkene C1-Ir and C8-Ir bonds lengths are 2.152(11) and 2.187(10) Å, respectively, and compare with those of 2.1664(13) and 2.1494(14) Å in $(\eta^2\text{-}COE)(Me)Ir(PMe_3)_3$[33] and 2.2865(7) and 2.307(7) Å in [(^{i}PrN-PCP)IrHCl(COE)][34]. The Ir-N_1 and Ir-N_2 bond lengths of **2** are 2.216(9) and 2.106(8) Å respectively in accordance with the *trans*-labilizing influence of hydride and compare with those of

2.192(3) and 2.129(3) Å in $[Ir(H)_2IMes(py)_3]Cl$ for sites *trans* to hydride and carbene, respectively.[35]

The ^1H NMR spectrum of **2** contains hydride ligand signals at δ –19.34 and –26.47 for sites *trans* to py and chloride respectively and two inequivalent CH proton signals for the COE ligand at δ 3.12 and 4.12. The ^{15}N chemical shifts of its py ligands appear at $\delta_{py\text{-}eq}$ 254.7 and $\delta_{py\text{-}ax}$ 224.7, with the former exhibiting a large $J_H{}^{15}{}_N$ splitting of 20 Hz due to a *trans* hydride ligand coupling. Diagnostic α-proton signals for these ligands appear at δ 9.37 and δ 9.25 respectively, with the low field ^{15}N axial py chemical shift reflecting its shorter iridium bond length.[36]

The ligands of **2** proved to exhibit dynamic effects that were quantified by exchange spectroscopy (EXSY) methods (Supporting Information). The rate of py loss for the equatorial site was determined to be 7.8 ± 0.1 s^{-1} at 298 K, and hydride site exchange into free H_2 proved to be limited at this temperature. In contrast, the two distinct hydride sites of **2** proved to interchange positions at a rate of 3.6 ± 0.1 s^{-1}, while the CH proton sites of COE interconvert at a rate of 3.8 ± 0.1 s^{-1}. When the concentrations of py and H_2 were varied (see sTable 1) none of the associated ligand exchange rates changed. Further samples were then examined that contained excesses of COE and Cl^- (in the form of $[^tBu_4C]Cl$) in addition to py and H_2 and no change in rate was observed. Hence py dissociation from the site *trans* to hydride forms $IrCl(H)_2(\eta^2\text{-}COE)(py)$ (**3**) of Scheme 1 with equivalent hydrides. For symmetry reasons, reformation of **2** proceeds with interchange of the original hydride and alkene CH proton sites at approximately 50% of the py loss rate. In agreement with this conclusion, Eyring analysis of this behavior as a function of temperature produces three slopes with identical gradients. The corresponding activation parameters for py loss are: $\Delta H^{\neq}$ = 90.6 ± 1 kJ mol^{-1} and $\Delta S^{\neq}$ = 79 ± 4 J K^{-1} mol^{-1} and reflect the dissociative nature of this change.

When the H_2 gas used in these control experiments was replaced by D_2, loss of the hydride ligand signals of **2** was observed over a few seconds with slow ^2H incorporation into the bound cyclooctene CH= groups being evident at a rate of 1.3 (± 0.5) x 10^{-5} s^{-1}. Furthermore, when *p*-H_2 is used, the corresponding hydride ligand signals exhibit the PHIP effect as detailed in Figure 2. These observations confirm that **2** undergoes reversible H_2 loss and when the same sample was exposed to *p*-H_2 in low magnetic field for 10 s prior to making the high-field NMR measurement the SABRE effect was observed. Figure 2b shows this when viewed through the 11 to –1 ppm region of the NMR spectrum for a sample containing one equivalent of free py relative to **2**. The bound py and COE protons signals referred to earlier are now hyperpolarized and consequently **2** is a SABRE catalyst.

The degree of SABRE shown in these resonances depends on the excess of py. When the initial ratio of **1** to py was 1 : 8, a > 210 fold intensity gain in the *ortho* proton resonance of the free py signal is observed. This enhancement increases to > 500 when the ligand ratio is 1: 5.6 and can be increased further by warming to 313; sTable 4 contains data for nicotinamide, nicotine, 5-aminopyrimidine and 3,5-lutudine to demonstrate scope. However, after leaving the sample at 298 K for 24 hours, three new hydride signals appear in the corresponding ^1H NMR spectra at δ –24.72, –25.9 and –28.95 for **4**. Their intensity growth parallels a series of changes in the aromatic region of these NMR spectra which suggest **4** contains four distinct py-based ligands. Integration and COSY measurements show that one of these has just four protons and hence **4** is the C-H bond activation product $(Cl)(H)(py)(\mu\text{-}Cl)(\mu\text{-}H)(\kappa\text{-}\mu\text{-}NC_5H_4)Ir(H)(py)_2$ of Figure 3.

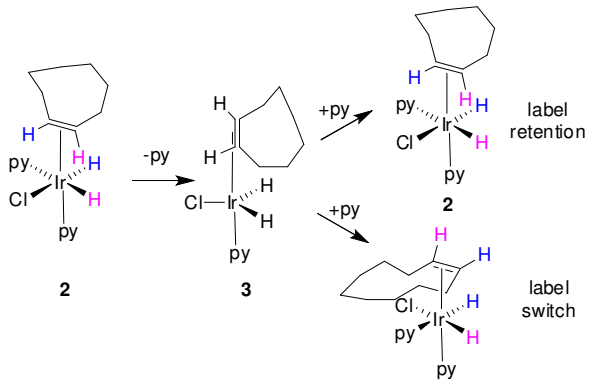

Scheme 1. Ligand exchange pathways observed by NMR for $IrCl(H)_2(COE)(Py)_2$ (**2**) in THF-d_8 solution.

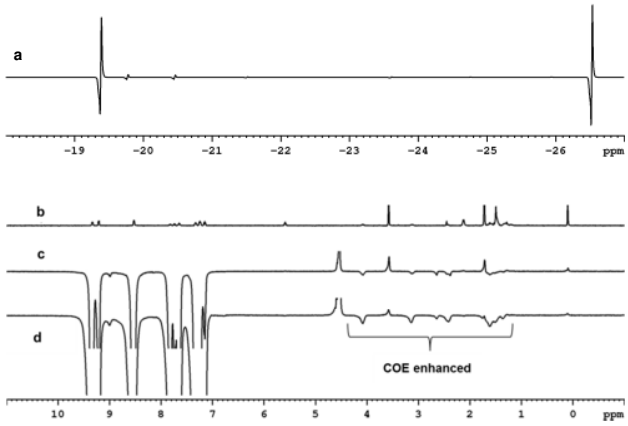

Figure 2: Hyperpolarized ^1H NMR spectra of **2**. (a) Hydride region showing PHIP enhanced signals for *cis-cis* **2** and its minor *cis-trans* isomer (298 K); Organic region: (b) the normal spectrum, (c) SABRE enhanced free and bound py signals (298 K) and (d) SABRE enhanced signals for the COE ligand of **2** (313 K).

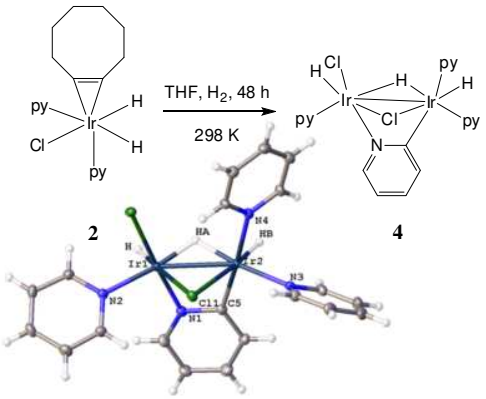

Figure 3. Reaction scheme for the formation of $(Cl)(H)(py)(\mu\text{-}Cl)(\mu\text{-}H)(\kappa\text{-}\mu\text{-}NC_5H_4)Ir(H)(py)_2$ (**4**) alongside an ORTEP of **4**.

The distance between the two iridium centers of **4** is 2.73319(18) Å while the corresponding Ir-C and Ir-N bond lengths of the bridging pyridyl moiety are 1.998(3) Å and 2.013 (3) Å respectively. A related iridium dimer studied by Cotton *et al.*[37] had analogous Ir-C, and Ir-N, bond lengths of 1.983(13) Å and 2.024(12) Å with an Ir-Ir distance of 2.518(1) Å. Our $Ir_1\text{-}N_2$, $Ir_1\text{-}Cl_2$ and $Ir_1\text{-}Cl_1$ bond lengths are 2.068(3) Å, 2.3897(8) Å and 2.5732(8) Å respectively in accordance with asymmetry in the bridging chloride. The corresponding $Ir_2\text{-}N_4$, $Ir_2\text{-}N_3$ and terminal

Ir_2-Cl_2 bond lengths are 2.152(3) Å, 2.072(3) Å and 2.5579(8) Å respectively with the hydride ligands again clearly exhibiting a *trans* labializing influence although the Ir-N bond lengths are all shorter than those of the labile site in **2**. The key bond angles for Ir_1 are N_2-Ir_1-Cl_2, Cl_2-Ir_1-Cl_1 and N_1-Ir_1-Cl_1 and 86.92(8)°, 93.72(3)° and 84.45(8)° respectively, while those for Ir_2, N_3-Ir_2-Cl_1, C_5-Ir_2-Cl_1 and N_4-Ir_2-Cl_1, are 98.53(8)°, 85.38(10)° and 92.89(8)°. The ligand arrangement around both iridium centers is close to octahedral.

Complex **4** is SABRE inactive and its hydride ligand signals fail to exhibit PHIP. However, shaken with **2** under *p*-H_2 the ^{1}H NMR signals of free py are enhanced alongside those for the bound py ligands of **4** which provide *ortho* proton signals at δ 9.48 and δ 9.40 which suggests ligand exchange is possible. The addition of pyridine-d_5 to the ^{1}H-labelled **4** under H_2 at 273 K confirms this effect, with the order of ligand exchange based on the fall in *ortho* proton site resonance intensities being δ 9.40 > δ 9.48 >> δ 9.33 as detailed in Figure 4. The corresponding Ir-N bond lengthens for these groups are 2.068(3) Å, 2.072(3) Å and 2.152(3) respectively and fit with these observations. Exchange of the pyridyl ligand with pyridine-d_5 proved to be slower still.

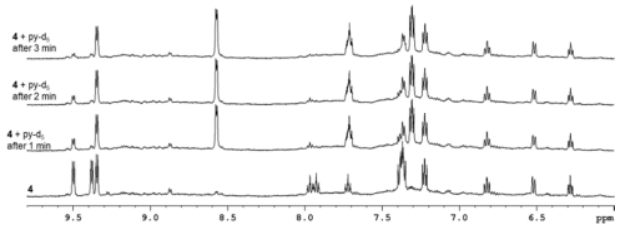

Figure 4. The intensity fall of appropriate ^{1}H NMR resonances in ^{1}H-containing **4** at 273 K upon exposure to pyridine-d_5 reveals the slow and selective exchange of its py based ligands.

In addition to these changes, the slow replacement of the ^{2}H labels of pyridine-d_5 with ^{1}H nuclei is seen. After 48 h at 313 K, 33 % of its *ortho* py ^{2}H sites became ^{1}H containing, with 5.4 % incorporation into the *para* site and 3.1 % into the *meta* site. **4** therefore causes py CH/CD exchange through transfer from D_2/H_2.[12] When 3 bars of D_2 was employed with a pyridine-h_5 to **4** ratio of 25:1, the rate of ^{2}H label incorporation proved to be 4.3 x 10^{-5} s^{-1} (*ortho*), 3.85 x 10^{-5} s^{-1} (*meta*), 3.05 x 10^{-5} s^{-1} (*para*) at 313 K.

Given the SABRE activity of $[Ir(H)_2(PCy_3)(py)_3][BF_4]$ referred to earlier, we added $AgPF_6$ to **2** to form $[Ir(H)_2(COE)(py)_3][PF_6]$ (**6**) of Scheme 2. **6** was also prepared independently from $[Ir(COE)_2(py)_2]PF_6$ (**5**) (Supporting Information). It proved to be SABRE-inactive at 298 K, in agreement with the py loss rate of 0.007 s^{-1}; warming to 313 K produces limited SABRE, but the bound py signals are stronger than those of free py. **6** is therefore unsuited to SABRE, the small ligand loss rate being consistent with the reduced steric effect of this ligand relative to PCy_3.

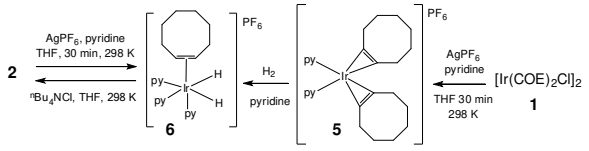

Scheme 2. Routes to $[Ir(H)_2(\eta^2\text{-cyclooctene})(py)_3][PF_6]$ (**6**).

In summary we have established that readily available air stable $[IrCl(COE)_2]_2$ (**1**) reacts with py and H_2 to form $IrCl(H)_2(\eta^2\text{-COE})(py)_2$, **2**. **2** is highly effective for the hyperpolarization of py via the SABRE effect in non-protoic solvents and with its simple alkene co-ligand far easier to employ than the carbene complexes more usually used. When this process is undertaken with nicotinamide, nicotine, 5-aminopyrimidine and 3,5-lutudine good levels of SABRE are seen. Hence **1** reflects a simple and readily available precatayst for this process.

Over 48 hrs, **2** reacts to form the novel C-H bond activation product $(Cl)(H)(py)(\mu\text{-}Cl)(\mu\text{-}H)(\kappa\text{-}\mu\text{-}NC_5H_4)Ir(H)(py)_2$ (**4**) in a reaction inhibited by added py. This novel complex exhibits catalytic activity in the HIE reaction which is used for the site-specific labelling of drugs. The presented results offer insight into the HIE process and suggest how ligand design might be used to improve its efficiency in the future. In addition, the high-field one-proton PHIP effect of Eisenberg[38] uses the chemical transfer of a single proton previously located in a molecule of *p*-H_2 to enable its detection as a hyperpolarized signal in an organic species.[38,39] While slow reacting **4** does not behave in this way, its detection suggests faster reacting systems with show PHIP at high-field.[40]

ASSOCIATED CONTENT

Supporting Information

The Supporting Information is availalbe free of charge on the ACS Publications website at DOI: 10.1021/acs.inorgchem.6b02560.

Complex synthesis and NMR spectra (PDF)
X-ray crystallographic data in CIF format for **2** (CIF)
X-ray crystallographic data in CIF format for **4** (CIF)
X-ray crystallographic data in CIF format for **5** (CIF)

AUTHOR INFORMATION

Corresponding Author

*Email: simon.duckett@york.ac.uk

Notes

The authors declare no competing financial interests.

ACKNOWLEDGMENT

We thank the Wellcome Trust for funding (grants 092506 and 098335).

REFERENCES

1. Albert, M. S.; Cates, G. D.; Driehuys, B.; Happer, W.; Saam, B.; Springer, C. S.; Wishnia, A. Biological Magnetic-Resonance-Imaging Using Laser Polarized Xe-129. *Nature* **1994,** 370 (6486), 199-201 DOI: 10.1038/370199a0.

2. Ardenkjaer-Larsen, J. H.; Fridlund, B.; Gram, A.; Hansson, G.; Hansson, L.; Lerche, M. H.; Servin, R.; Thaning, M.; Golman, K. Increase in signal-to-noise ratio of > 10,000 times in liquid-state NMR. *Proc. Natl. Acad. Sci. U. S. A.* **2003,** 100 (18), 10158-10163 DOI: 10.1073/pnas.1733835100.

3. Bowers, C. R.; Weitekamp, D. P. Para-Hydrogen and Synthesis Allow Dramatically Enhanced Nuclear Alignment. *J. Am. Chem. Soc.* **1987,** 109 (18), 5541-5542 DOI: 10.1021/ja00252a049.

4. Kurhanewicz, J.; Vigneron, D. B.; Brindle, K.; Chekmenev, E. Y.; Comment, A.; Cunningham, C. H.; DeBerardinis, R. J.; Green, G. G.; Leach, M. O.; Rajan, S. S.; Rizi, R. R.; Ross, B. D.; Warren, W. S.; Malloy, C. R. Analysis of Cancer Metabolism by Imaging Hyperpolarized Nuclei: Prospects for Translation to Clinical Research. *Neoplasia* **2011,** 13 (2), 81-97 DOI: 10.1593/neo.101102.

5. Green, R. A.; Adams, R. W.; Duckett, S. B.; Mewis, R. E.; Williamson, D. C.; Green, G. G. R. The theory and practice of hyperpolarization in magnetic resonance using parahydrogen. *Prog. Nucl. Magn. Reson. Spectrosc.* **2012,** 67, 1-48 DOI: 10.1016/j.pnmrs.2012.03.001.

6. Eisenschmid, T. C.; Kirss, R. U.; Deutsch, P. P.; Hommeltoft, S. I.; Eisenberg, R.; Bargon, J.; Lawler, R. G.; Balch, A. L. Para Hydrogen Induced Polarization in Hydrogenation Reactions. *J. Am. Chem. Soc.* **1987,** 109 (26), 8089-8091 DOI: 10.1021/ja00260a026.
7. Natterer, J.; Bargon, J. Parahydrogen induced polarization. *Prog. Nucl. Magn. Reson. Spectrosc.* **1997,** 31, 293-315 DOI: 10.1016/s0079-6565(97)00007-1.
8. Chekmenev, E. Y.; Hovener, J.; Norton, V. A.; Harris, K.; Batchelder, L. S.; Bhattacharya, P.; Ross, B. D.; Weitekamp, D. P. PASADENA hyperpolarization of succinic acid for MRI and NMR spectroscopy. *J. Am. Chem. Soc.* **2008,** 130 (13), 4212-+ DOI: 10.1021/ja7101218.
9. Hasnip, S. K.; Duckett, S. B.; Sleigh, C. J.; Taylor, D. R.; Barlow, G. K.; Taylor, M. J. New products in an old reaction: isomeric products from H-2 addition to Vaska's complex and its analogues. *Chem. Commun. (Cambridge, U. K.)* **1999,** (17), 1717-1718 DOI: 10.1039/a905590h.
10. Adams, R. W.; Aguilar, J. A.; Atkinson, K. D.; Cowley, M. J.; Elliott, P. I. P.; Duckett, S. B.; Green, G. G. R.; Khazal, I. G.; Lopez-Serrano, J.; Williamson, D. C. Reversible Interactions with para-Hydrogen Enhance NMR Sensitivity by Polarization Transfer. *Science* **2009,** 323 (5922), 1708-1711 DOI: 10.1126/science.1168877.
11. Crabtree, R. IRIDIUM COMPOUNDS IN CATALYSIS. *Acc. Chem. Res.* **1979,** 12 (9), 331-338 DOI: 10.1021/ar50141a005.
12. Ellames, G. J.; Gibson, J. S.; Herbert, J. M.; McNeill, A. H. The scope and limitations of deuteration mediated by Crabtree's catalyst. *Tetrahedron* **2001,** 57 (46), 9487-9497 DOI: 10.1016/s0040-4020(01)00945-0.
13. Nilsson, G. N.; Kerr, W. J. The development and use of novel iridium complexes as catalysts for ortho-directed hydrogen isotope exchange reactions. *J. Labelled Compd. Radiopharm.* **2010,** 53 (11-12), 662-667 DOI: 10.1002/jlcr.1817.
14. Atkinson, K. D.; Cowley, M. J.; Elliott, P. I. P.; Duckett, S. B.; Green, G. G. R.; Lopez-Serrano, J.; Whitwood, A. C. Spontaneous Transfer of Parahydrogen Derived Spin Order to Pyridine at Low Magnetic Field. *J. Am. Chem. Soc.* **2009,** 131 (37), 13362-13368 DOI: 10.1021/ja903601p.
15. Lloyd, L. S.; Asghar, A.; Burns, M. J.; Charlton, A.; Coombes, S.; Cowley, M. J.; Dear, G. J.; Duckett, S. B.; Genov, G. R.; Green, G. G. R.; Highton, L. A. R.; Hooper, A. J. J.; Khan, M.; Khazal, I. G.; Lewis, R. J.; Mewis, R. E.; Roberts, A. D.; Ruddlesden, A. J. Hyperpolarisation through reversible interactions with parahydrogen. *Catal. Sci. Tech.* **2014,** 4 (10), 3544-3554 DOI: 10.1039/c4cy00464g.
16. Eshuis, N.; Hermkens, N.; van Weerdenburg, B. J. A.; Feiters, M. C.; Rutjes, F.; Wijmenga, S. S.; Tessari, M. Toward Nanomolar Detection by NMR Through SABRE Hyperpolarization. *J. Am. Chem. Soc.* **2014,** 136 (7), 2695-2698 DOI: 10.1021/ja412994k.
17. Theis, T.; Truong, M. L.; Coffey, A. M.; Shchepin, R. V.; Waddell, K. W.; Shi, F.; Goodson, B. M.; Warren, W. S.; Chekmenev, E. Y. Microtesla SABRE Enables 10% Nitrogen-15 Nuclear Spin Polarization. *J. Am. Chem. Soc.* **2015,** 137 (4), 1404-1407 DOI: 10.1021/ja512242d.
18. Truong, M. L.; Theis, T.; Coffey, A. M.; Shchepin, R. V.; Waddell, K. W.; Shi, F.; Goodson, B. M.; Warren, W. S.; Chekmenev, E. Y. N-15 Hyperpolarization by Reversible Exchange Using SABRE-SHEATH. *J. Phys. Chem. C* **2015,** 119 (16), 8786-8797 DOI: 10.1021/acs.jpcc.5b01799.
19. Lloyd, L. S.; Adams, R. W.; Bernstein, M.; Coombes, S.; Duckett, S. B.; Green, G. G. R.; Lewis, R. J.; Mewis, R. E.; Sleigh, C. J. Utilization of SABRE-Derived Hyperpolarization To Detect Low-Concentration Analytes via 1D and 2D NMR Methods. *J. Am. Chem. Soc.* **2012,** 134 (31), 12904-12907 DOI: 10.1021/ja3051052.
20. Eshuis, N.; van Weerdenburg, B. J. A.; Feiters, M. C.; Rutjes, F.; Wijmenga, S. S.; Tessari, M. Quantitative Trace Analysis of Complex Mixtures Using SABRE Hyperpolarization. *Angew. Chem., Int. Ed.* **2015,** 54 (5), 1481-1484 DOI: 10.1002/anie.201409795.
21. Mewis, R. E.; Atkinson, K. D.; Cowley, M. J.; Duckett, S. B.; Green, G. G. R.; Green, R. A.; Highton, L. A. R.; Kilgour, D.; Lloyd, L. S.; Lohman, J. A. B.; Williamson, D. C. Probing signal amplification by reversible exchange using an NMR flow system. *Magn. Reson. Chem.* **2014,** 52 (7), 358-369 DOI: 10.1002/mrc.4073.
22. Zhivonitko, V. V.; Skovpin, I. V.; Koptyug, I. V. Strong P-31 nuclear spin hyperpolarization produced via reversible chemical interaction with parahydrogen. *Chem. Commun. (Cambridge, U. K.)* **2015,** 51 (13), 2506-2509 DOI: 10.1039/c4cc08115c.
23. van Weerdenburg, B. J. A.; Gloggler, S.; Eshuis, N.; Engwerda, A. H. J.; Smits, J. M. M.; de Gelder, R.; Appelt, S.; Wymenga, S. S.; Tessari, M.; Feiters, M. C.; Blumich, B.; Rutjes, F. Ligand effects of NHC-iridium catalysts for signal amplification by reversible exchange (SABRE). *Chem. Commun. (Cambridge, U. K.)* **2013,** 49 (67), 7388-7390 DOI: 10.1039/c3cc43423k.
24. Barskiy, D. A.; Shchepin, R. V.; Coffey, A. M.; Theis, T.; Warren, W. S.; Goodson, B. M.; Chekmenev, E. Y. Over 20% N-15 Hyperpolarization in Under One Minute for Metronidazole, an Antibiotic and Hypoxia Probe. *J. Am. Chem. Soc.* **2016,** 138 (26), 8080-8083 DOI: 10.1021/jacs.6b04784.
25. Logan, A. W. J.; Theis, T.; Colell, J. F. P.; Warren, W. S.; Malcolmson, S. J. Hyperpolarization of Nitrogen-15 Schiff Bases by Reversible Exchange Catalysis with para-Hydrogen. *Chem. Eur. J.* **2016,** 22 (31), 10777-10781 DOI: 10.1002/chem.201602393.
26. Zeng, H. F.; Xu, J. D.; Gillen, J.; McMahon, M. T.; Artemov, D.; Tyburn, J. M.; Lohman, J. A. B.; Mewis, R. E.; Atkinson, K. D.; Green, G. G. R.; Duckett, S. B.; van Zijl, P. C. M. Optimization of SABRE for polarization of the tuberculosis drugs pyrazinamide and isoniazid. *J. Magn. Reson.* **2013,** 237, 73-78 DOI: 10.1016/j.jmr.2013.09.012.
27. Mewis, R. E.; Green, R. A.; Cockett, M. C. R.; Cowley, M. J.; Duckett, S. B.; Green, G. G. R.; John, R. O.; Rayner, P. J.; Williamson, D. C. Strategies for the Hyperpolarization of Acetonitrile and Related Ligands by SABRE. *J. Phys. Chem. B* **2015,** 119 (4), 1416-1424 DOI: 10.1021/jp511492q.
28. Ducker, E. B.; Kuhn, L. T.; Munnemann, K.; Griesinger, C. Similarity of SABRE field dependence in chemically different substrates. *J. Magn. Reson.* **2012,** 214, 159-165 DOI: 10.1016/j.jmr.2011.11.001.
29. Vazquez-Serrano, L. D.; Owens, B. T.; Buriak, J. M. Catalytic olefin hydrogenation using N-heterocyclic carbene-phosphine complexes of iridium. *Chem. Commun. (Cambridge, U. K.)* **2002,** (21), 2518-2519 DOI: 10.1039/b208403a.
30. Adams, R. W.; Duckett, S. B.; Green, R. A.; Williamson, D. C.; Green, G. G. R. A theoretical basis for spontaneous polarization transfer in non-hydrogenative parahydrogen-induced polarization. *J. Chem. Phys.* **2009,** 131 (19), 15 DOI: 10.1063/1.3254386.
31. Eshuis, N.; Aspers, R.; van Weerdenburg, B. J. A.; Feiters, M. C.; Rutjes, F.; Wijmenga, S. S.; Tessari, M. Determination of long-range scalar H-1-H-1 coupling constants responsible for polarization transfer in SABRE. *J. Magn. Reson.* **2016,** 265, 59-66 DOI: 10.1016/j.jmr.2016.01.012.
32. Nelson, D. J.; Truscott, B. J.; Slawin, A. M. Z.; Nolan, S. P. Synthesis and Reactivity of New Bis(N-heterocyclic carbene) Iridium(I) Complexes. *Inorg. Chem.* **2013,** 52 (21), 12674-12681 DOI: 10.1021/ic4018773.
33. Bleeke, J. R.; Thananatthanachon, T.; Rath, N. P. Silapentadienyl−Iridium−Phosphine Chemistry. *Organometallics* **2008,** 27 (11), 2436-2446 DOI: 10.1021/om800041b.
34. Brück, A.; Gallego, D.; Wang, W.; Irran, E.; Driess, M.; Hartwig, J. F. Pushing the σ-Donor Strength in Iridium Pincer Complexes: Bis(silylene) and Bis(germylene) Ligands Are Stronger Donors than Bis(phosphorus(III)) Ligands. *Angew. Chem. Int. Ed. Engl.* **2012,** 51 (46), 11478-11482 DOI: 10.1002/anie.201205570.
35. Cowley, M. J.; Adams, R. W.; Atkinson, K. D.; Cockett, M. C. R.; Duckett, S. B.; Green, G. G. R.; Lohman, J. A. B.; Kerssebaum, R.; Kilgour, D.; Mewis, R. E. Iridium N-Heterocyclic Carbene Complexes as Efficient Catalysts for Magnetization Transfer from para-Hydrogen. *J. Am. Chem. Soc.* **2011,** 133 (16), 6134-6137 DOI: 10.1021/ja200299u.
36. Pazderski, L. Application of N-15 NMR Spectroscopy to Determine Coordination Sphere Geometry in Pd(II), Pt(II), Pt(IV), CO(III) and Rh(III) Complexes with Azines. *Pol. J. Chem.* **2009,** 83 (7), 1241-1253.
37. Cotton, F. A.; Poli, R. Synthesis and Molecular-Structure of a Dinuclear Quadruply Bridged Cobalt(Ii) Compound with a Short Metal Metal Bond, Co2[(P-Ch3c6h4)Nnnp-C6h4ch3)]4. *Inorg. Chem.* **1987,** 26 (22), 3652-3653 DOI: Doi 10.1021/Ic00269a006.
38. Permin, A. B.; Eisenberg, R. One-hydrogen polarization in hydroformylation promoted by platinum-tin and iridium carbonyl complexes: A new type of parahydrogen-induced effect. *J. Am. Chem. Soc.* **2002,** 124 (42), 12406-12407 DOI: 10.1021/ja026698t.

39. Lopez-Serrano, J.; Duckett, S. B.; Aiken, S.; Lenero, K. Q. A.; Drent, E.; Dunne, J. P.; Konya, D.; Whitwood, A. C. A para-hydrogen investigation of palladium-catalyzed alkyne hydrogenation. *J. Am. Chem. Soc.* **2007,** 129 (20), 6513-6527 DOI: 10.1021/ja070331c.
40. Barskiy, D. A.; Kovtunov, K. V.; Koptyug, I. V.; He, P.; Groome, K. A.; Best, Q. A.; Shi, F.; Goodson, B. M.; Shchepin, R. V.; Coffey, A. M.; Waddell, K. W.; Chekmenev, E. Y. The Feasibility of Formation and Kinetics of NMR Signal Amplification by Reversible Exchange (SABRE) at High Magnetic Field (9.4 T). *J. Am. Chem. Soc.* **2014,** 136 (9), 3322-3325 DOI: 10.1021/ja501052p.

For Table of Contents Only

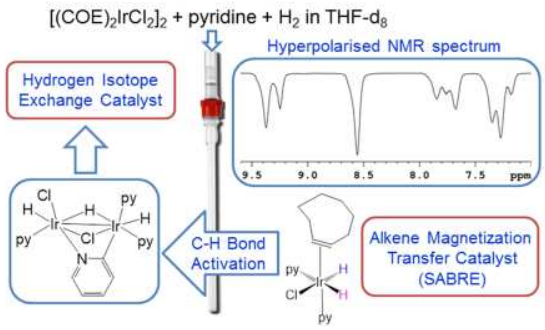

$[IrCl(COE)_2]_2$ reacts to form $IrCl(H)_2(COE)(py)_2$ with pyridine and H_2 which undergoes py loss to form 16-electron $IrCl(H)_2(COE)(py)$ with equivalent hydride ligands. When studied with *para*hydrogen, it efficiently achieves the hyperpolarization of free py (and nicotinamide, nicotine, 5-aminopyrimidine and 3,5-lutudine) but forms $(Cl)(H)(py)(\mu\text{-}Cl)(\mu\text{-}H)(\kappa\text{-}\mu\text{-}NC_5H_4)Ir(H)(py)_2$ with py over 48 hrs which is active in the hydrogen isotope exchange process.